

## Four $N^7$ -alkoxybenzyl-substituted 4,5,6,7-tetrahydro-1*H*-pyrazolo[3,4-*b*]pyridine-5-spiro-1'-cyclohexane-2',6'-diones: hydrogen-bonded supramolecular structures in zero, one, two or three dimensions

Jorge Trilleras,<sup>a</sup> Jairo Quiroga,<sup>a</sup> Justo Cobo,<sup>b</sup> John N. Low<sup>c</sup> and Christopher Glidewell<sup>d\*</sup>

<sup>a</sup>Grupo de Investigación de Compuestos Heterocíclicos, Departamento de Química, Universidad de Valle, AA 25360, Cali, Colombia, <sup>b</sup>Departamento de Química Inorgánica y Orgánica, Universidad de Jaén, 23071 Jaén, Spain, <sup>c</sup>Department of Chemistry, University of Aberdeen, Meston Walk, Old Aberdeen AB24 3UE, Scotland, and <sup>d</sup>School of Chemistry, University of St Andrews, Fife KY16 9ST, Scotland

Correspondence e-mail: cg@st-andrews.ac.uk

Received 18 November 2008

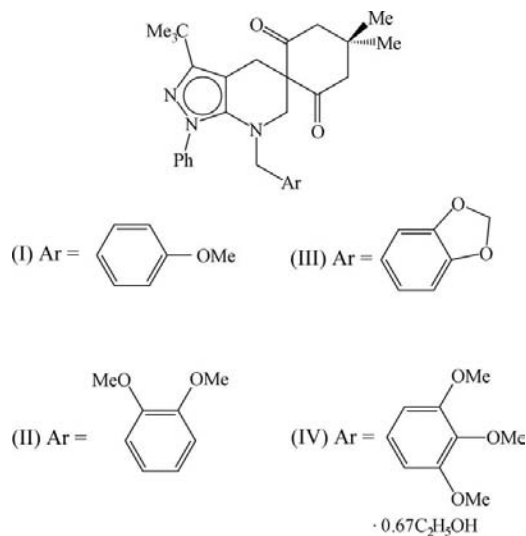
Accepted 19 November 2008

Online 27 November 2008

3-*tert*-Butyl-7-(4-methoxybenzyl)-4',4'-dimethyl-1-phenyl-4,5,6,7-tetrahydro-1*H*-pyrazolo[3,4-*b*]pyridine-5-spiro-1'-cyclohexane-2',6'-dione,  $C_{31}H_{37}N_3O_3$ , (I), 3-*tert*-butyl-7-(2,3-dimethoxybenzyl)-4',4'-dimethyl-1-phenyl-4,5,6,7-tetrahydro-1*H*-pyrazolo[3,4-*b*]pyridine-5-spiro-1'-cyclohexane-2',6'-dione,  $C_{32}H_{39}N_3O_4$ , (II), 3-*tert*-butyl-4',4'-dimethyl-7-(3,4-methylenedioxybenzyl)-1-phenyl-4,5,6,7-tetrahydro-1*H*-pyrazolo[3,4-*b*]pyridine-5-spiro-1'-cyclohexane-2',6'-dione,  $C_{31}H_{35}N_3O_4$ , (III), and 3-*tert*-butyl-4',4'-dimethyl-1-phenyl-7-(3,4,5-trimethoxybenzyl)-4,5,6,7-tetrahydro-1*H*-pyrazolo[3,4-*b*]pyridine-5-spiro-1'-cyclohexane-2',6'-dione ethanol 0.67-solvate,  $C_{33}H_{41}N_3O_5 \cdot 0.67C_2H_6O$ , (IV), all contain reduced pyridine rings having half-chair conformations. The molecules of (I) and (II) are linked into centrosymmetric dimers and simple chains, respectively, by C—H...O hydrogen bonds, augmented only in (I) by a C—H... $\pi$  hydrogen bond. The molecules of (III) are linked by a combination of C—H...O and C—H... $\pi$  hydrogen bonds into a chain of edge-fused centrosymmetric rings, further linked by weak hydrogen bonds into supramolecular arrays in two or three dimensions. The heterocyclic molecules in (IV) are linked by two independent C—H...O hydrogen bonds into sheets, from which the partial-occupancy ethanol molecules are pendent. The significance of this study lies in its finding of a very wide range of supramolecular aggregation modes dependent on rather modest changes in the peripheral substituents remote from the main hydrogen-bond acceptor sites.

### Comment

In continuation of our structural study of  $N^7$ -benzyl-substituted pyrazolo[3,4-*b*]pyridine-5-spiro-1'-cyclohexane-2',6'-diones (Cruz *et al.*, 2008) – itself part of a programme exploring the use of multicomponent condensation reactions, especially those induced by microwave irradiation under solvent-free conditions, for the synthesis of novel heterocycles – we now report the molecular and supramolecular structures of four  $N^7$ -alkoxybenzyl derivatives, (I)–(IV) (Figs. 1–4). Compounds (I)–(IV) were synthesized using the reaction between a substituted *N*-benzylaminopyrazole, 5,5-dimethylcyclohexane-1,3-dione (dimedone) and excess paraformaldehyde, under solvent-free conditions, in a straightforward modification of the synthetic method employed by Cruz *et al.* (2008).



Compounds (I)–(III) crystallized in solvent-free form, but compound (IV) was found to be a partial ethanol solvate, with 0.67 molecules of ethanol per molecule of the pyrazolopyridine in the crystal selected for data collection. We have not investigated systematically the stoichiometry of this solvate, but it is possible that different individual crystals might yield somewhat different values for the occupancy of the ethanol sites. Equally it is possible that for any such crystal, exposure to the X-ray beam might cause progressive loss of the ethanol component over time or that the occupancy of the ethanol sites throughout a crystal so exposed to X-rays may become spatially inhomogeneous, or that both effects may be present. Such spacial and/or temporal variation in the ethanol occupancy, with the associated degradation of the crystal quality, might well be expected to compromise the quality of the refinement indicators. Examination using *PLATON* (Spek, 2003) of the refined structure of (IV), but with the ethanol component omitted, found eight voids, each of volume *ca* 96 Å<sup>3</sup> and together accounting for some 12.2% of the unit-cell volume. It is possible that the ethanol of solvation is present in this structure merely as a placeholder component, occupying what would otherwise be empty space.

In each compound, the reduced pyridine ring adopts a half-chair conformation, as shown (Table 1) by the ring-puckering parameters (Cremer & Pople, 1975), defined here for the

atom-sequence N7—C6—C5—C4—C3A—C7A. For an idealized half-chair ring with equal bond lengths throughout, the ring-puckering angles are  $\theta = 50.8^\circ$  and  $\varphi = (60k + 30)^\circ$ , where  $k$  represents an integer.

The rest of the molecular conformation is determined by the orientation of the three pendent substituents relative to the heterocyclic molecular core, and by the orientation of the alkoxy substituents relative to the adjacent aryl ring (Table 1). As indicated by the relevant torsion angles (Table 1), while the orientation of the phenyl and benzyl units relative to the molecular core is fairly similar in each compound, there is considerable variation in the degree to which the *tert*-butyl group has been rotated about the C3—C31 bond. Since the rotational barrier about this bond approximates to a sixfold barrier, as found when a fragment of local  $C_3$  symmetry, such as a *tert*-butyl group, is bonded to a fragment with effective local  $C_2$  symmetry, such as a planar ring, it can be expected that the barrier is exceptionally low, no more than a few tens of Joules per mole (Tannenbaum *et al.*, 1956; Naylor & Wilson, 1957), so accounting for the variation in the relative orientation of the *tert*-butyl group.

The orientations of the methoxy substituents in (I), (II) and (IV) show some interesting variations. As shown by the relevant torsion angles (Table 1), the single methoxy group in (I), that at C73 in (II), and those at C73 and C75 in (IV) are all almost coplanar with the adjacent aryl rings. The deviations from the mean planes of these rings are 0.235 (3) Å for atom C741 in (I), 0.006 (3) Å for atom C731 in (II), and 0.147 (5) and 0.164 (5) Å for atoms C731 and C751, respectively, in

(IV). Associated with each of these effectively in-plane methoxy groups is a marked difference between the two exocyclic C—C—O angles, typically almost  $10^\circ$ . By contrast, the C74/O74/C741 plane in (IV) is almost orthogonal to the adjacent ring, with atom C741 displaced by 1.058 (5) Å from

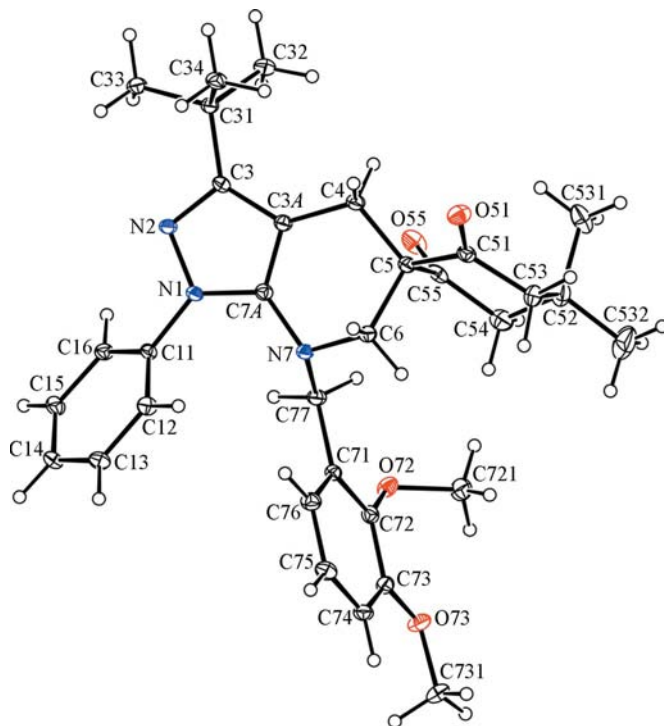


**Figure 2**  
The molecular structure of (II). Displacement ellipsoids are drawn at the 30% probability level.

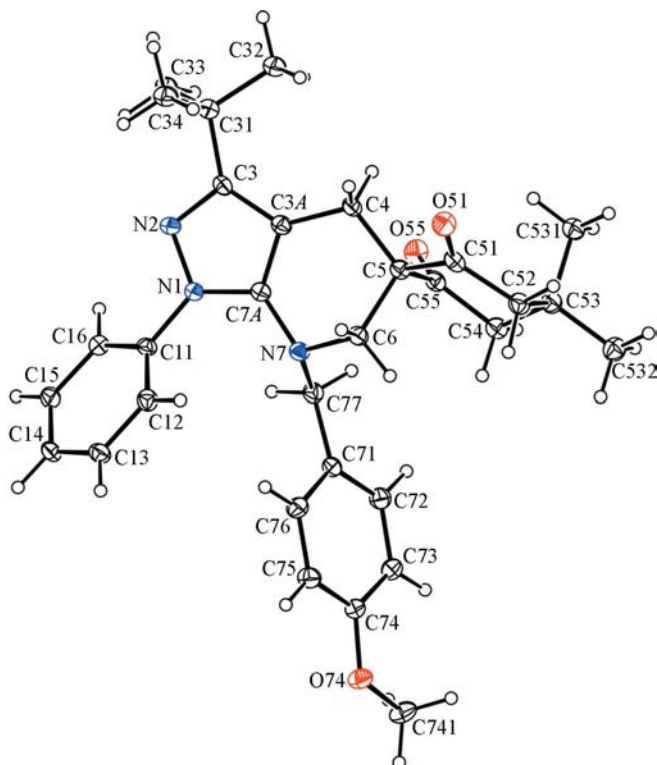


**Figure 1**  
The molecular structure of (I). Displacement ellipsoids are drawn at the 30% probability level.

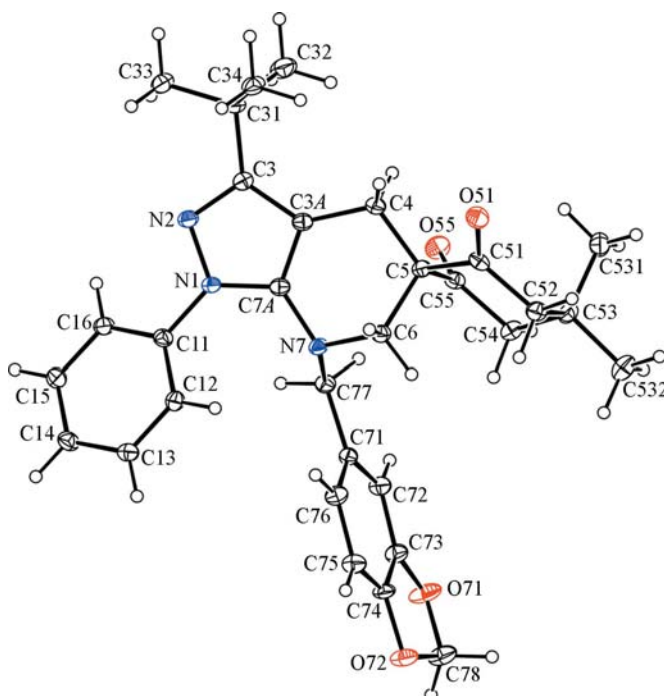


**Figure 3**  
The molecular structure of (III). Displacement ellipsoids are drawn at the 30% probability level.

the ring plane, while atom C721 in (II) is displaced from the adjacent ring plane by 0.944 (3) Å. At the same time, in (IV), the exocyclic C–C–O angles at atom C74 are identical within experimental uncertainty, and those at atom C72 in (II) differ by less than 3°. Although the in-plane conformation appears to be the most favoured and of lowest energy, maximizing the orbital overlap between the  $\pi$  orbitals of the ring and formally nonbonding  $2p$  orbital on the O atom, this orientation is nonetheless rather easily disrupted by nonbonded (steric) interactions between adjacent substituents. In (III), the five-membered ring formed by the methylenedioxy unit adopts an envelope conformation, folded across the line O71···O72.

Although compounds (I)–(IV) all contain potential hydrogen-bond acceptors – in the methoxy groups in (I), (II) and (IV), and in the methylenedioxy unit in (III) – in no case do these O atoms play any significant role in the supramolecular aggregation. There is a rather long C–H···O contact involving such an O atom in (III) (Table 2), although this is possibly only of marginal structural significance, at best, while the methoxy O atoms in the other three compounds do not form even weak contacts of this type. The principal intermolecular interactions in this series are of C–H··· $\pi$  type and of C–H···O type utilizing carbonyl O atoms as the hydrogen-bond acceptors. There are no  $\pi$ – $\pi$  stacking interactions in any of (I)–(IV). The partial-occupancy ethanol component in (IV) is connected to the heterocyclic component by a three-point linkage (Table 2), but it plays no role in the supramolecular aggregation, acting simply as a pendent group.

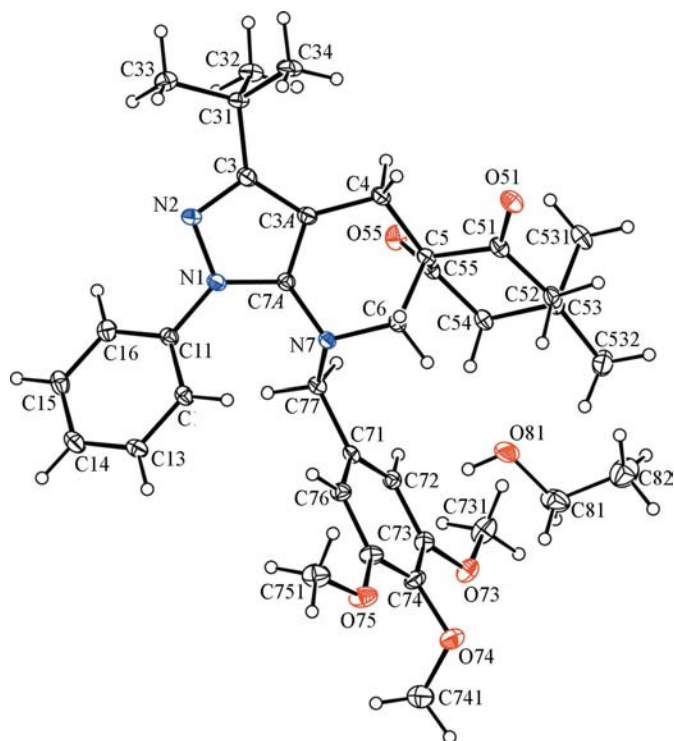
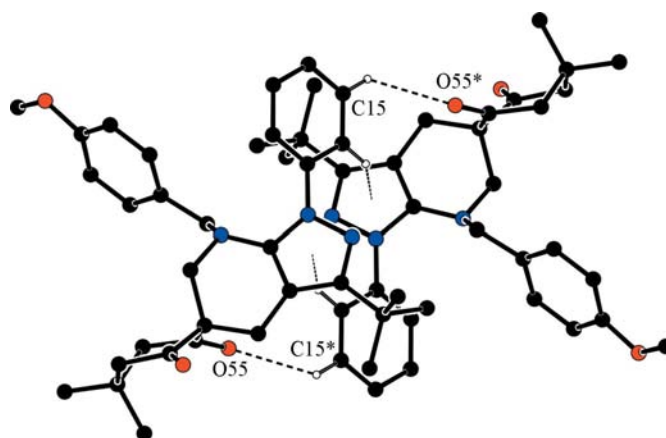


**Figure 4**  
The molecular structure of (IV). The ethanol component has occupancy 0.670 (7) (see *Experimental*). Displacement ellipsoids are drawn at the 30% probability level.

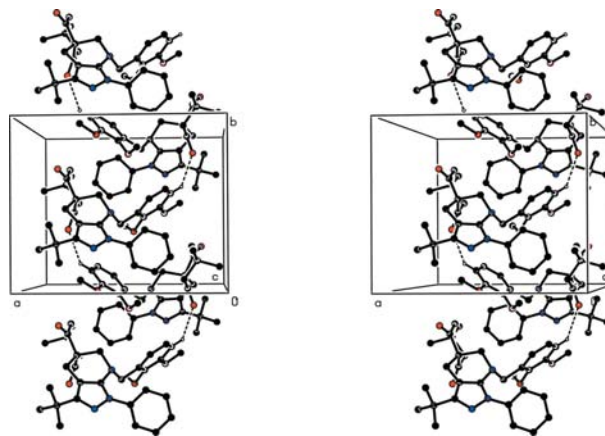
In compound (I), pairs of molecules are linked by the cooperative action of C–H···O and C–H··· $\pi$  hydrogen bonds into centrosymmetric dimers, within which the paired C–H···O hydrogen bonds define an  $R_2^2(22)$  (Bernstein *et al.*, 1995) motif (Fig. 5), but there are no direction-specific interactions between these dimers; hence the supramolecular aggregation in compound (I) can be regarded as finite, or zero-dimensional.

A single C–H···O hydrogen bond links molecules of (II), which are related by the  $2_1$  screw axis along  $(\frac{1}{2}, y, \frac{3}{4})$ , into a simple  $C(11)$  chain running parallel to the [010] direction (Fig. 6). Two chains of this type related to one another by inversion pass through each unit cell, but there are no direction-specific interactions between adjacent chains.

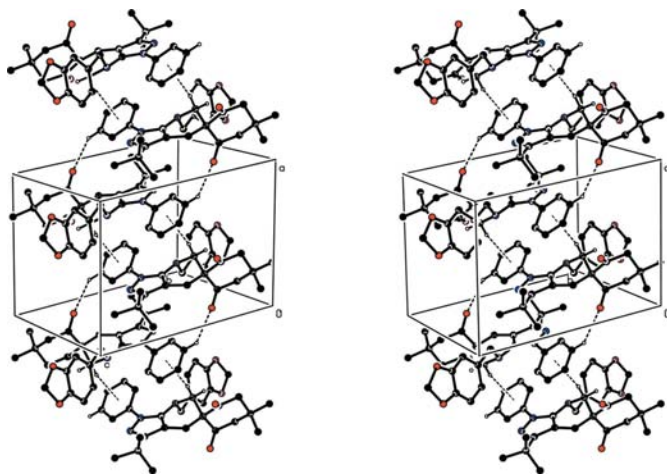
In (III), a combination of a C–H···O hydrogen bond, with C15 as the donor, and a C–H··· $\pi$  hydrogen bond links the molecules into a chain of centrosymmetric edge-fused rings running parallel to the [100] direction (Fig. 7). Within this chain,  $R_2^2(22)$  rings exactly analogous to those observed in (I)



**Figure 5**  
Part of the crystal structure of (I), showing the formation of a centrosymmetric dimer. For the sake of clarity, H atoms not involved in the motifs shown have been omitted. Atoms marked with an asterisk (\*) are at the symmetry position  $(-x, 1-y, 1-z)$ .



**Figure 6**  
A stereoview of part of the crystal structure of (II), showing the formation of a  $C(11)$  chain along [010]. For the sake of clarity, H atoms not involved in the motif shown have been omitted.

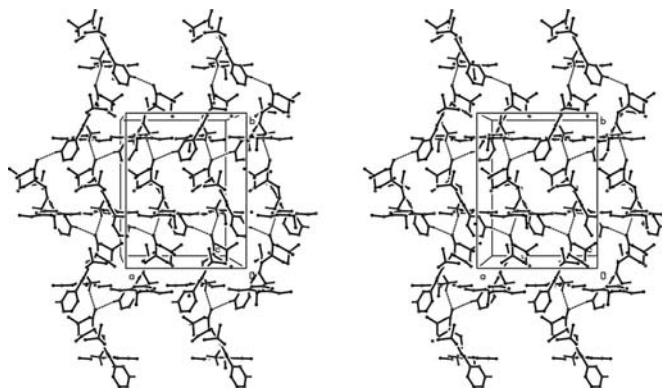

**Figure 7**

A stereoview of part of the crystal structure of (III), showing the formation of a chain along [100] containing two types of centrosymmetric ring. For the sake of clarity, H atoms bonded to C atoms not involved in the motifs shown have been omitted.

are centred at  $(n, \frac{1}{2}, \frac{1}{2})$ , where  $n$  represents an integer, and these alternate with rings formed by pairs of C—H... $\pi$  hydrogen bonds, centred at  $(n + \frac{1}{2}, \frac{1}{2}, \frac{1}{2})$ , where  $n$  represents zero or an integer. Within the structure of (III), there are two further C—H...O contacts, both rather long, and it is of interest to examine their possible structural effects. The interaction involving C13 as the donor links the chains of rings, which are related by translation along [010], while that involving C72 as the donor links the  $R_2^2(22)$  rings into a chain along [001]. Thus, if these two interactions are regarded as structurally significant, the supramolecular structure is based on the one-dimensional chains of rings along [100] (Fig. 7), which become successively linked into two-dimensional and three-dimensional arrays.

The heterocyclic components in (IV) are linked into a sheet by two C—H...O hydrogen bonds, both utilizing the same carbonyl acceptor atom, and the formation of the sheet is readily analysed in terms of the individual actions of the two hydrogen bonds. The aryl atom C13 at  $(x, y, z)$  acts as a hydrogen-bond donor to carbonyl atom O51 at  $(-x, -\frac{1}{2} + y, \frac{1}{2} - z)$ , so linking molecules related by the  $2_1$  screw axis along  $(0, y, \frac{1}{4})$ , and so forming a  $C(11)$  chain running parallel to the [010] direction. In the second substructure, methylene atom C77 at  $(x, y, z)$  acts as a hydrogen-bond donor to atom O51 at  $(\frac{1}{2} - x, -\frac{1}{2} + y, z)$ , thus linking molecules related by the  $b$ -glide plane at  $x = \frac{1}{4}$  into a  $C(7)$  chain, again running parallel to the [010] direction. The combination of these two chain motifs generates a sheet of  $R_4^3(28)$  rings lying parallel to (001) (Fig. 8) and occupying the domain  $0 < z < \frac{1}{2}$ . A second sheet, related to the first by inversion, occupies the domain  $\frac{1}{2} < z < 1$ , but there are no direction-specific interactions between adjacent sheets. As noted above, the partial-occupancy ethanol molecules are absent from this sheet, but they play no role in its formation.

Although the methoxy substituents in (I), (II) and (IV) play no direct role in the supramolecular aggregation, it is striking


**Figure 8**

A stereoview of part of the crystal structure of (IV), showing the formation of a sheet parallel to (001). For the sake of clarity, the partial-occupancy ethanol component and H atoms bonded to C atoms not involved in the motifs shown have been omitted.

that, as the degree of methoxy substitution increases, so too does the dimensionality of the hydrogen-bonded structure, from zero-dimensional in the monomethoxy compound (I) to one-dimensional in the dimethoxy compound (II) to two-dimensional in the trimethoxy compound (IV). It is interesting to note that the variations in the molecular constitution occur solely in the substituted benzyl ring, which is, of course, remote from the main hydrogen-bond acceptor sites, the carbonyl O atoms and the main hydrogen-bond donor sites, most of which are provided by the unsubstituted phenyl ring.

## Experimental

Microwave-induced syntheses were carried out using a focused microwave reactor (CEM Discover TM). A mixture of the appropriately substituted *N*-benzylaminopyrazole (2 mmol), 5,5-dimethylcyclohexane-1,3-dione (2 mmol) and an excess of paraformaldehyde (80–100 mg) was exposed to microwave radiation at 473 K with a maximum power of 300 W for 25 min. The reaction mixtures were dissolved in hot ethanol. After cooling these solutions, the solid products were collected by filtration and washed with ethanol and then with hexane ( $2 \times 5$  ml) to afford the pure products. Colourless crystals suitable for single-crystal X-ray diffraction were grown by slow evaporation of solutions in ethanol. For (I), yield 75%, m.p. 445–447 K; HRMS found 499.2835,  $C_{31}H_{37}N_3O_3$  requires 499.2835. For (II), yield 85%, m.p. 503–505 K; HRMS found 529.2941,  $C_{32}H_{39}N_3O_4$  requires 529.2941. For (III), yield 70%, m.p. 475–477 K; HRMS found 513.2635,  $C_{31}H_{35}N_3O_4$  requires 513.2628. For (IV), yield 71%, m.p. 456–458 K; HRMS found 559.3032,  $C_{33}H_{41}N_3O_5$  requires 559.3046.

## Compound (I)

### Crystal data

$C_{31}H_{37}N_3O_3$	$\gamma = 87.216 (7)^\circ$
$M_r = 499.64$	$V = 1304.7 (3) \text{ \AA}^3$
Triclinic, $P\bar{1}$	$Z = 2$
$a = 9.5971 (8) \text{ \AA}$	Mo $K\alpha$ radiation
$b = 11.2549 (16) \text{ \AA}$	$\mu = 0.08 \text{ mm}^{-1}$
$c = 12.1452 (14) \text{ \AA}$	$T = 120 (2) \text{ K}$
$\alpha = 86.979 (11)^\circ$	$0.51 \times 0.36 \times 0.18 \text{ mm}$
$\beta = 85.487 (10)^\circ$	



**Table 1**

Selected geometric parameters (Å, °) for (I)–(IV).

(a) Ring-puckering parameters for the atom sequence N7–C6–C5–C4–C3A–C7A

Parameter	(I)	(II)	(III)	(IV)
$Q$	0.441 (3)	0.450 (2)	0.426 (3)	0.460 (4)
$\theta$	50.5 (4)	50.3 (3)	51.6 (4)	53.6 (5)
$\varphi$	80.8 (4)	86.0 (4)	72.2 (4)	81.6 (6)

(b) Torsion angles

	(I)	(II)	(III)	(IV)
N2–C3–C31–C32	–165.1 (2)	–127.3 (2)	–127.3 (3)	–103.6 (4)
N2–C3–C31–C33	–43.4 (3)	–7.0 (3)	–6.5 (4)	16.2 (5)
N2–C3–C31–C34	74.5 (3)	112.8 (2)	113.3 (3)	136.9 (4)
N2–N1–C11–C12	–133.8 (2)	–130.9 (2)	–149.1 (3)	–138.5 (3)
C6–N7–C77–C71	69.7 (3)	72.0 (2)	66.8 (3)	59.8 (4)
N7–C77–C71–C72	–143.6 (2)	–156.3 (2)	–156.8 (2)	–131.5 (3)
C71–C72–O72–C721	–	125.3 (2)	–	–
C72–C73–O73–C731	–	177.0 (2)	–	5.6 (5)
C73–C74–O74–C741	–5.3 (4)	–	–	–88.9 (5)
C76–C75–O75–C751	–	–	–	4.0 (6)
C72–C73–O71–C78	–	–	170.3 (3)	–
C75–C74–O72–C78	–	–	–170.5 (3)	–

(c) Bond angles

	(I)	(II)	(III)	(IV)
C71–C72–O72	–	118.5 (2)	–	–
C73–C72–O72	–	120.9 (2)	–	–
C72–C73–O73	–	115.9 (2)	–	123.9 (3)
C74–C73–O73	–	124.3 (2)	–	115.5 (3)
C73–C74–O74	124.7 (2)	–	–	120.0 (3)
C75–C74–O74	115.6 (2)	–	–	120.4 (3)
C74–C75–O75	–	–	–	115.2 (3)
C76–C75–O75	–	–	–	124.6 (3)

**Data collection**

Bruker–Nonius KappaCCD diffractometer  
Absorption correction: multi-scan (SADABS; Sheldrick, 2003)  
 $T_{\min} = 0.971$ ,  $T_{\max} = 0.985$   
36057 measured reflections

**Refinement**

$R[F^2 > 2\sigma(F^2)] = 0.060$   
 $wR(F^2) = 0.199$   
 $S = 1.04$   
5986 reflections  
340 parameters

5986 independent reflections  
3281 reflections with  $I > 2\sigma(I)$   
 $R_{\text{int}} = 0.081$

H-atom parameters constrained  
 $\Delta\rho_{\text{max}} = 0.31 \text{ e } \text{Å}^{-3}$   
 $\Delta\rho_{\text{min}} = -0.39 \text{ e } \text{Å}^{-3}$

**Compound (II)****Crystal data**

$\text{C}_{32}\text{H}_{30}\text{N}_3\text{O}_4$   
 $M_r = 529.66$   
Monoclinic,  $P2_1/c$   
 $a = 12.4683 (15) \text{ Å}$   
 $b = 10.2892 (12) \text{ Å}$   
 $c = 21.7635 (16) \text{ Å}$   
 $\beta = 90.843 (10)^\circ$

$V = 2791.7 (5) \text{ Å}^3$   
 $Z = 4$   
Mo  $K\alpha$  radiation  
 $\mu = 0.08 \text{ mm}^{-1}$   
 $T = 120 (2) \text{ K}$   
 $0.32 \times 0.25 \times 0.12 \text{ mm}$

**Table 2**

Hydrogen bonds and short intermolecular contacts (Å, °) for (I)–(IV).

Compound	$D\cdots H\cdots A$	$D\cdots H$	$H\cdots A$	$D\cdots A$	$D\cdots H\cdots A$
(I)	C15–H15 $\cdots$ O55 <sup>i</sup>	0.95	2.54	3.229 (3)	130
	C16–H16 $\cdots$ Cg1 <sup>1<i>a</i></sup>	0.95	2.88	3.589 (3)	132
(II)	C74–H74 $\cdots$ O55 <sup>ii</sup>	0.95	2.47	3.256 (3)	140
(III)	C13–H13 $\cdots$ O51 <sup>iii</sup>	0.95	2.58	3.182 (3)	121
	C15–H15 $\cdots$ O55 <sup>iv</sup>	0.95	2.46	3.173 (3)	132
	C72–H72 $\cdots$ O71 <sup>v</sup>	0.95	2.60	3.503 (3)	160
	C6–H6A $\cdots$ Cg2 <sup>vi,b</sup>	0.99	2.69	3.670 (3)	169
(IV)	O81–H81 $\cdots$ Cg2 <sup>b</sup>	0.84	2.69	3.423 (4)	147
	C6–H6A $\cdots$ O81	0.99	2.58	3.406 (6)	141
	C52–H52A $\cdots$ O81	0.99	2.48	3.470 (6)	174
	C13–H13 $\cdots$ O51 <sup>vii</sup>	0.95	2.43	3.194 (5)	137
	C77–H77B $\cdots$ O51 <sup>viii</sup>	0.99	2.45	3.193 (4)	131

Notes: (a) Cg1 represents the centroid of the N1/N2/C3/C3A/C7A ring; (b) Cg2 represents the centroid of the C71–C76 ring. Symmetry codes: (i)  $-x, -y + 1, -z + 1$ ; (ii)  $-x + 1, y + \frac{1}{2}, -z + \frac{3}{2}$ ; (iii)  $x, y - 1, z$ ; (iv)  $-x + 2, -y + 1, -z + 1$ ; (v)  $-x + 2, -y + 1, -z + 2$ ; (vi)  $-x + 1, -y + 1, -z + 1$ ; (vii)  $-x, y - \frac{1}{2}, -z + \frac{1}{2}$ ; (viii)  $-x + \frac{1}{2}, y - \frac{1}{2}, z$ .

**Data collection**

Bruker–Nonius KappaCCD diffractometer  
Absorption correction: multi-scan (SADABS; Sheldrick, 2003)  
 $T_{\min} = 0.965$ ,  $T_{\max} = 0.990$   
45254 measured reflections

6394 independent reflections  
4404 reflections with  $I > 2\sigma(I)$   
 $R_{\text{int}} = 0.065$

**Refinement**

$R[F^2 > 2\sigma(F^2)] = 0.061$   
 $wR(F^2) = 0.138$   
 $S = 1.18$   
6394 reflections

359 parameters  
H-atom parameters constrained  
 $\Delta\rho_{\text{max}} = 0.28 \text{ e } \text{Å}^{-3}$   
 $\Delta\rho_{\text{min}} = -0.31 \text{ e } \text{Å}^{-3}$

**Compound (III)****Crystal data**

$\text{C}_{31}\text{H}_{35}\text{N}_3\text{O}_4$   
 $M_r = 513.62$   
Triclinic,  $P\bar{1}$   
 $a = 9.2691 (14) \text{ Å}$   
 $b = 11.0898 (11) \text{ Å}$   
 $c = 12.802 (2) \text{ Å}$   
 $\alpha = 92.844 (10)^\circ$   
 $\beta = 95.185 (12)^\circ$

$\gamma = 91.070 (11)^\circ$   
 $V = 1308.6 (3) \text{ Å}^3$   
 $Z = 2$   
Mo  $K\alpha$  radiation  
 $\mu = 0.09 \text{ mm}^{-1}$   
 $T = 120 (2) \text{ K}$   
 $0.54 \times 0.29 \times 0.10 \text{ mm}$

**Data collection**

Bruker–Nonius KappaCCD diffractometer  
Absorption correction: multi-scan (SADABS; Sheldrick, 2003)  
 $T_{\min} = 0.964$ ,  $T_{\max} = 0.991$   
36798 measured reflections

6010 independent reflections  
2954 reflections with  $I > 2\sigma(I)$   
 $R_{\text{int}} = 0.129$

**Refinement**

$R[F^2 > 2\sigma(F^2)] = 0.063$   
 $wR(F^2) = 0.171$   
 $S = 1.06$   
6010 reflections

348 parameters  
H-atom parameters constrained  
 $\Delta\rho_{\text{max}} = 0.31 \text{ e } \text{Å}^{-3}$   
 $\Delta\rho_{\text{min}} = -0.34 \text{ e } \text{Å}^{-3}$

## Compound (IV)

### Crystal data

$C_{33}H_{41}N_3O_5 \cdot 0.67C_2H_6O$	$V = 6328.0 (15) \text{ \AA}^3$
$M_r = 590.55$	$Z = 8$
Orthorhombic, <i>Pbca</i>	Mo $K\alpha$ radiation
$a = 13.5770 (17) \text{ \AA}$	$\mu = 0.08 \text{ mm}^{-1}$
$b = 17.476 (3) \text{ \AA}$	$T = 120 (2) \text{ K}$
$c = 26.670 (3) \text{ \AA}$	$0.32 \times 0.32 \times 0.28 \text{ mm}$

### Data collection

Bruker–Nonius KappaCCD diffractometer	53340 measured reflections
Absorption correction: multi-scan (SADABS; Sheldrick, 2003)	7255 independent reflections
$T_{\min} = 0.974$ , $T_{\max} = 0.977$	4959 reflections with $I > 2\sigma(I)$
	$R_{\text{int}} = 0.058$

### Refinement

$R[F^2 > 2\sigma(F^2)] = 0.087$	407 parameters
$wR(F^2) = 0.206$	H-atom parameters constrained
$S = 1.17$	$\Delta\rho_{\text{max}} = 0.59 \text{ e \AA}^{-3}$
7255 reflections	$\Delta\rho_{\text{min}} = -0.36 \text{ e \AA}^{-3}$

For (II) and (IV), the space groups  $P2_1/c$  and  $Pbca$ , respectively, were uniquely assigned from the systematic absences. Crystals of (I) and (III) are triclinic; for each, the space group  $P\bar{1}$  was selected and then confirmed by the structure analysis. All H atoms were located in difference maps and then treated as riding atoms in geometrically idealized positions, with C–H distances of 0.95 (aromatic), 0.98 (CH<sub>3</sub>) or 0.99 Å (CH<sub>2</sub>) and an O–H distance of 0.84 Å, and with  $U_{\text{iso}}(\text{H}) = kU_{\text{eq}}(\text{carrier})$ , where  $k = 1.5$  for the methyl and hydroxy H atoms, and  $k = 1.2$  for all other H atoms. In the crystal of (IV) selected for data collection, the site occupancy for the ethanol component refined to a value of 0.670 (7). Crystals of (III) diffracted rather weakly, even at 120 K, with only 49% of the data labelled ‘observed’; the merging index was also fairly high, at 0.129. The crystals of (IV) consistently exhibited internal fissures, and all attempts to cut small fragments from larger crystals resulted in destruction and the formation of powdery residues. This behaviour is certainly consistent with progressive loss of the ethanol component. The data set collected for compound (IV) appeared to be entirely satisfactory, as judged by the data completeness (99.7% at  $\theta = 27.51^\circ$ ), the merging index, and the precision of the unit-cell dimensions. However, the refinement converged at a rather high  $R$  value, with a fairly large linear term in the weighting scheme. Scrutiny of the resulting interatomic distances and the  $U_{ij}$  values in compound (IV), and comparison with the corresponding parameters in compounds (I)–(III) showed no anomalies. In the crystal selected for data collection, the occupancy of the ethanol site refined to 0.670 (7) but, as noted in the *Comment* section, it is possible that different individual crystals might yield somewhat different values for the occupancy of the

ethanol sites. Subsequent examination of the original frames showed some diffuse diffraction streaks, again consistent with degradation of the crystal quality, even at 120 K. Attempts to crystallize compound (IV) from an alternative solvent (dimethylformamide) gave no crystalline material.

For all compounds, data collection: *COLLECT* (Hooft, 1999); cell refinement: *DIRAX/LSQ* (Duisenberg *et al.*, 2000); data reduction: *EVALCCD* (Duisenberg *et al.*, 2003); program(s) used to solve structure: *SIR2004* (Burla *et al.*, 2005); program(s) used to refine structure: *OSCAIL* (McArdle, 2003) and *SHELXL97* (Sheldrick, 2008); molecular graphics: *PLATON* (Spek, 2003); software used to prepare material for publication: *SHELXL97* and *PRPKAPPA* (Ferguson, 1999).

The authors thank ‘Servicios Técnicos de Investigación of Universidad de Jaén’ and the staff for data collection. JC thanks the Consejería de Innovación, Ciencia y Empresa (Junta de Andalucía, Spain) and the Universidad de Jaén for financial support. JT and JQ thank COLCIENCIAS and UNIVALLE (Universidad del Valle, Colombia) for financial support.

Supplementary data for this paper are available from the IUCr electronic archives (Reference: SK3276). Services for accessing these data are described at the back of the journal.

## References

- Bernstein, J., Davis, R. E., Shimoni, L. & Chang, N.-L. (1995). *Angew. Chem. Int. Ed. Engl.* **34**, 1555–1573.
- Burla, M. C., Caliandro, R., Camalli, M., Carrozzini, B., Cascarano, G. L., De Caro, L., Giacovazzo, C., Polidori, G. & Spagna, R. (2005). *J. Appl. Cryst.* **38**, 381–388.
- Cremer, D. & Pople, J. A. (1975). *J. Am. Chem. Soc.* **97**, 1354–1358.
- Cruz, S., Trilleras, J., Cobo, J., Low, J. N. & Glidewell, C. (2008). *Acta Cryst.* **C64**, o637–o642.
- Duisenberg, A. J. M., Hooft, R. W. W., Schreurs, A. M. M. & Kroon, J. (2000). *J. Appl. Cryst.* **33**, 893–898.
- Duisenberg, A. J. M., Kroon-Batenburg, L. M. J. & Schreurs, A. M. M. (2003). *J. Appl. Cryst.* **36**, 220–229.
- Ferguson, G. (1999). *PRPKAPPA*. University of Guelph, Canada.
- Hooft, R. W. W. (1999). *COLLECT*. Nonius BV, Delft, The Netherlands.
- McArdle, P. (2003). *OSCAIL for Windows*. Version 10. Crystallography Centre, Chemistry Department, NUI Galway, Ireland.
- Naylor, R. E. & Wilson, E. B. (1957). *J. Chem. Phys.* **26**, 1057–1060.
- Sheldrick, G. M. (2003). *SADABS*. Version 2.10. University of Göttingen, Germany.
- Sheldrick, G. M. (2008). *Acta Cryst.* **A64**, 112–122.
- Spek, A. L. (2003). *J. Appl. Cryst.* **36**, 7–13.
- Tannenbaum, E., Myers, R. J. & Gwinn, W. D. (1956). *J. Chem. Phys.* **25**, 42–47.